Antibody Catalyzed Hydrolysis of Enol Ethers

Jean-Louis Reymond,* Guiti K. Jahangiri, Catherine Stoudt, and Richard A. Lerner*

Contribution from the Department of Molecular Biology, The Scripps Research Institute, 10666 North Torrey Pines Road, La Jolla, California 92037

Received December 17, 1992

Abstract: The hydrolysis of alkyl enol ethers to their corresponding carbonyl compounds proceeds by rate determining protonation of the β-carbon to form an activated oxocarbonium ion intermediate and is catalyzed by acids (Kresge, A. J.; Chiang, Y. *J. Chem. Soc. B* **1967**, 53). It can be catalyzed by antibodies with very high enantioselectivity of protonation at the β-carbon to form optically pure carbonyl compounds (Reymond, J.-L.; Janda, K. D.; Lerner, R. A. *J. Am. Chem. Soc.* **1992**, *114*, 2257). In the present study, the pH profile of the antibody 14D9 (*anti*-**1**) catalyzed, enantioselective hydrolysis of enol ether **4** between pH = 3.1 and pH = 7.2 has been measured in both H_2O and D_2O at 20 °C. The kinetic solvent isotope effect is $(k_H/k_D)_{cat}$ = 1.75 for the antibody catalyzed reaction and $(k_H/k_D)_{uncat}$ = 1.92 for the background reaction. The Michaelis–Menten constant K_m for substrate **4** changes from 35 μM at low pH to 190 μM at high pH. Saturation of the catalytic activity is observed at low pH. These observations are consistent with general acid catalysis by an ionizable side chain with pK = 5.2, presumably a carboxyl group, in the active site. A maximum rate acceleration k_{cat}/k_{uncat} = 8200 is obtained at the high pH end of the profile, and a maximum turnover number of 9.75×10^{-5} s^{-1} is obtained at the low pH end. Enol ethers **15–21** are also catalytically hydrolyzed by 14D9. The maximum turnover numbered measured is 0.39 s^{-1} with **17** at pH = 6.0 at 20 °C. The catalytic effect k_{cat}/k_{uncat} is influenced by the structure of the enol ether. Catalysis increases by a factor of 12 between **15** and its β-methyl analog **4** and by a factor of 34 between the six-membered ring enol ether **19** and its five-membered ring analog **17**. These rate effects may reflect the principle of strain in catalysis. They suggest that hydrophobic interactions directly participate in transition-state stabilization, which is unexpected for an acid–base reaction usually discussed in terms of proton relay mechanisms. The implication of these findings for the design and improvement of antibody catalysts is discussed.

Introduction

The relationship between structure and function of natural enzymes and proteins is extremely complex and makes the rational, de novo design of active proteins very difficult. As first suggested by Jencks in 1969[1] and demonstrated in 1986 by Lerner[2] and by Schultz,[2] a practical entry into designed catalysis is provided by antibodies raised against stable transition state analogs of chemical reactions. This approach is not only simple and practical but also appears to be very versatile in terms of reaction types and substrates.[2]

Because antibodies are optically pure proteins, they are particularly attractive for asymmetric catalysis of stereogenic transformations. Recently, we reported that antibodies raised against haptens **1**, **2**, and **3** catalyze the hydrolysis of enol ethers **4** and **5**[3] (Scheme I). For one of them (14D9, *anti*-**1**), the catalytic reaction was shown to proceed with very high enantioselectivity of protonation at the β-carbon atom, to yield nearly optically pure aldehyde **6**, with the same absolute configuration from both isomeric substrates **4** and **5**. This catalytic system has practical appeal for organic synthesis for the preparation of optically pure aldehydes and ketones by absolute, catalytic, asymmetric induction from an achiral substrate.

Acid catalyzed hydrolysis of **4** or **5** proceeds by rate determining proton transfer from an acid to the β-carbon to produce a highly reactive oxocarbonium ion **I** (Scheme I), which reacts with a water molecule to form a hemiacetal and finally aldehyde **6**. In the case of *anti*-**1** antibody 14D9, which was originally characterized for its ability to catalyze the hydrolysis of the glycoside model **7**[4] (Chart I), and later turned out to be one of the best

Scheme I. Structures of the Racemic Haptens **1**, **2** and **3**, Prochiral Enol Ether Substrates **4** and **5**, and Their Hydrolysis via Oxocarbonium Ion I

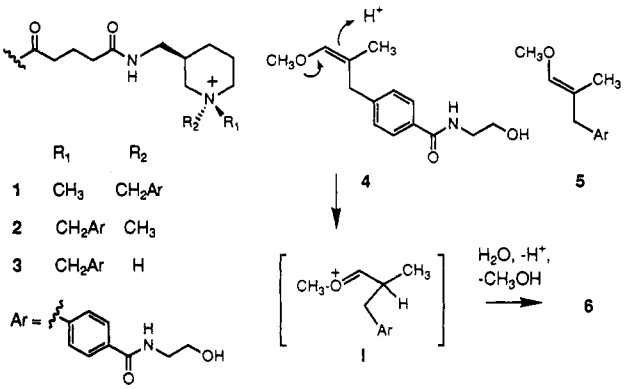

catalysts for the hydrolysis of enol ethers **4** and **5**, the relationship between hapten **1** and the reaction's transition state is not simple. For example, two structural features suggested by the mechanism do not appear in hapten **1**. First, and unlike in the tertiary amine **3**, the quaternary ammonium center in **1** does not contain an exchangeable hydrogen atom to mimic the crucial, rate determining proton transfer to the β-carbon. Second, the positively charged nitrogen atom is not substituted for the ether's oxygen atom that bears most of the charge in the transition state but instead for the β-carbon undergoing protonation.

We have now carried out a detailed study to understand which structural elements in **1** are important for catalysis, and therefore actually represent the transition state of the reaction in the immune response. We address the possibility of two effects to account for the catalysis of enol ether cleavage: (1) the presence of an ionizable protein side chain, elicited against the positive charge in the hapten, to act as a proton source and/or for electrostatic stabilization of the transition state; (2) binding interactions to the tetrahedral

(1) Jencks, W. *Catalysis in Chemistry and Enzymology*; McGraw-Hill: New York, 1969.
(2) Comprehensive review: Lerner, R. A.; Benkovic, P. G.; Schultz, P. G. *Science* **1991**, *252*, 659–667.
(3) Reymond, J.-L.; Janda, K. D.; Lerner, R. A. *J. Am. Chem. Soc.* **1992**, *114*, 2257.
(4) Reymond, J.-L.; Janda, K. D.; Lerner, R. A. *Angew. Chem., Int. Ed. Engl.* **1991**, *30*, 1711.

0002-7863/93/1515-3909$04.00/0

Chart I

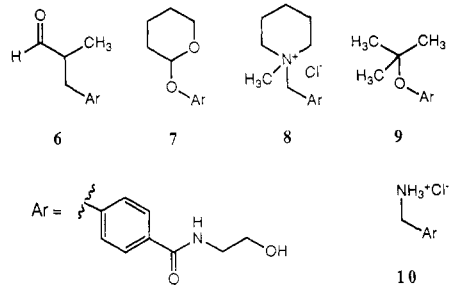

ammonium center to achieve substrate activation by pyramidalization of the β-carbon atom.

Results and Discussion

Active Site Titrations. When a catalytic reaction is observed with an antibody, inhibition of catalysis by the hapten used for immunization allows its assignment to the antibody combining site. Compound **8** (Chart I), an achiral analog of hapten **1**, is a tight binding inhibitor of antibody 14D9. Its dissociation constant is approximately 10^{-8} M at pH = 7.4, as estimated by competitive ELISA assay. All kinetic measurements reported here were performed at antibody active site concentrations of 2–5 × 10^{-6} M. At these concentrations, the free inhibitor concentration at 50% inhibition is therefore only 1% of the total inhibitor. In practice, a linear decrease of the catalytic activity of 14D9 down to zero is observed with increasing concentration of **8** and allows an accurate quantification of the active site concentration in an antibody preparation. The catalytic activity per milligram of antibody protein (measured by UV at 280 nm) was found to vary by more than 40% between different batches of the antibody. However, the catalytic activity per active site, measured by titration with compound **8**, was constant within 5%. Furthermore, the same active site concentration was obtained using different substrates as probes for the catalytic activity, confirming that the different catalytic activities observed originated in the same active site. Using substrate **4** as probe for the catalytic activity, titration with **8** was performed on one antibody sample in buffered 100% H_2O and 90% D_2O, and the apparent active site concentration was found to be identical in both cases. We therefore assumed that the activity of different antibody samples dyalized in either 100% H_2O or 100% D_2O could be reliably compared by titration with compound **8**. Active site titrations showed that the antibody was not measurably denaturing at low pH (pH = 3.1). All catalytic rates discussed here are related to the measured active site concentration of the antibody as determined by titration with **8**.

pH Profile. The values for antibody catalyzed hydrolysis of substrate **4** in buffered aqueous solution from pH 3 to pH 7 in H_2O and D_2O are reported in Table I. In both solvents, the K_m value changes from approximately 35 μM at low pH to approximately 190 μM at high pH (Figure 1). The shape of the pH dependence of K_m suggests that this pH-dependent transition is caused by the ionization of a protein side chain with pK value between 5 and 6. This is further confirmed by the approximately 0.4 pH units upward shift of the curve in D_2O which reflects a typical thermodynamic solvent isotope effect on the association constant of the side chain.[5] The same effect is seen in the pH dependence of k_{cat} (Figure 2), which shows a typical saturation behavior at low pH consistent with direct participation of the side chain in catalysis. As a higher affinity for the neutral substrate **4** is found at low pH in an active site induced by a positively charged hapten, this hypothetical side chain should be neutral in the protonated state and negatively charged as free base. Cysteine, tyrosine, serine, threonine, aspartate, and glutamate would fit this behavior but not histidine, arginine, or lysine.

(5) (a) Bunton, C. A.; Shiner, V. J. *J. Am. Chem. Soc.* **1961**, *83*, 42. (b) Salomaa, P.; Schaleger, L. L.; Long, F. A. *J. Am. Chem. Soc.* **1964**, *86*, 3.

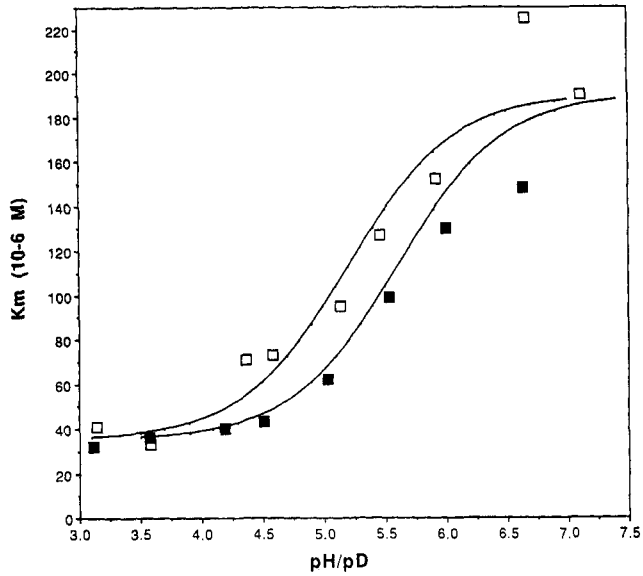

Figure 1. pH-profile of the Michaelis–Menten constant K_m for antibody 14D9 catalyzed hydrolysis of **4**: (□) values in H_2O and (■) values in D_2O. The lines were calculated from K_m = ([AbXH]/[Ab_{TOT}]) 35 μM + ([AbX^-]/[Ab_{TOT}]) 190 μM using pK_{XH} = 5.2 (H_2O) and pK_{XD} = 5.6 (D_2O).

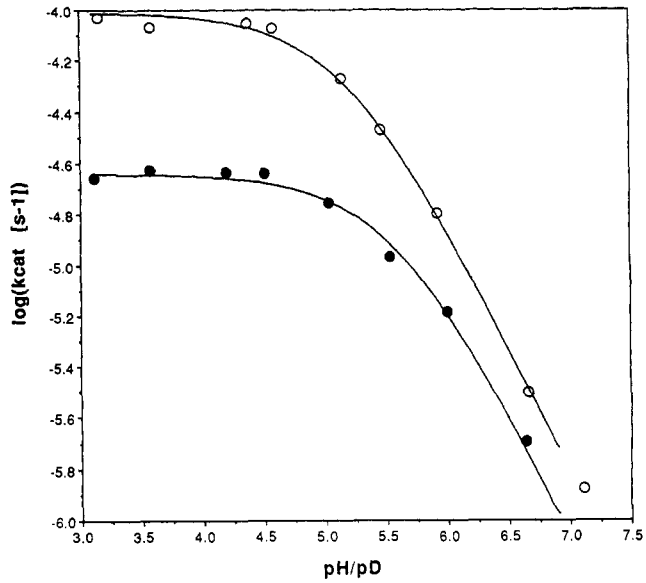

Figure 2. pH-profile of the catalytic constant as log(k_{cat}[s^{-1}]) for antibody 14D9 catalyzed hydrolysis of **4**: (○) values in H_2O and (●) values in D_2O. The lines were calculated from eq 7 or 8 (see text) using k_X (H_2O) = 15.5 M^{-1} s^{-1}, pK_{XH} = 5.2, and k_X (D_2O) = 8.85 M^{-1} s^{-1}, pK_{XD} = 5.6 as determined from the corresponding $1/k_{cat}$ vs $1/[H^+]$ plots.

Uncatalyzed Reaction. The uncatalyzed hydrolysis of **4**, referred to as "background reaction", is first order in hydronium ion concentration, with $k(H_3O^+)$ = 1.9 × 10^{-3} M^{-1} s^{-1} and $k(D_3O^+)$ = 9.9 × 10^{-4} M^{-1} s^{-1}. There is no measurable pH-independent, spontaneous reaction with the solvent water, within the pH-range studied. The substrate is completely stable under basic conditions (1 mM NaOH). A small amount of buffer catalysis is observed with citrate buffer. At the buffer concentration used (10 mM), it accounts for up to 10% of the total background reaction but has no effect on the antibody catalyzed reaction. These observations are consistent with the known aqueous chemistry of enol ethers.[6]

pH-Dependence of Antibody Catalysis. If we consider an antibody side-chain XH with dissociation constant K_{XH} in water (eq 1), the rate constant k_{cat} for the reaction of the antibody–substrate complex [Ab·S] (eq 2) is expected to be different in the two protonation states [AbXH·S] and [AbX^-·S]. In both states, the antibody–substrate complex can react to the product either

under hydronium ion catalysis in a pH-dependent process analogous to the background reaction or with a molecule of solvent water in a pH-independent process, by a yet unknown mechanism. The observation that k_{cat} becomes pH-independent at low pH, where the protonated antibody–substrate complex [AbXH·S] predominates, shows that there is no significant reaction of [AbXH·S] with hydronium ion. At high pH, where the ionized antibody–substrate complex [AbX⁻·S] predominates, k_{cat} becomes directly proportional to the hydronium ion concentration (slope of −1 in log(k_{cat}) vs pH plot). This suggests that there is no significant pH-independent reaction of [AbX⁻·S] within the pH range studied. To account for the experimental pH-rate profile of k_{cat}, we need to consider only the second-order reaction of [AbX⁻·S] with H_3O^+ and the first-order reaction of [AbXH·S]. The corresponding rate constants are k_{X^-} and k_{XH}, respectively (eqs 3 and 4). Because the protonation preequilibrium between [AbX⁻·S] and [AbXH·S] is much faster than the rate limiting step for the reaction of the antibody–substrate complex described by k_{cat}, both processes are kinetically equivalent; in fact, their rate constants k_{X^-} and k_{XH} are related to a description of the activation energy of the *same* reaction from two different thermodynamic reference states, namely the two ionization states of the antibody–substrate complex, [AbXH·S] and [AbX⁻·S], in buffered aqueous solution. This relation is also apparent in the proportionality relation between the dissociation constant of the antibody side chain K_{XH} and the two rate constants (eq 5). Combining eq 6 for the total side chain amount with eqs 1 and 3 gives eq 7 for the dependence of the catalytic constant on hydronium ion concentration in terms of the first order rate law. Equation 8 is the equivalent expression in terms of the second-order rate law. The same reasoning applies to the rates observed

$$K_{XH} = ([AbX^-][H_3O^+])/[AbXH] \quad (1)$$

$$Ab + S \overset{K_m}{\rightleftarrows} [Ab{\cdot}S] \overset{k_{cat}}{\rightarrow} P \quad (2)$$

$$k_{cat} = ([AbXH]/[Ab_{TOT}])k_{XH} \quad (3)$$

$$k_{cat} = [H_3O^+]([AbX^-]/[Ab_{TOT}])k_{X^-} \quad (4)$$

$$K_{XH} = k_{XH}/k_{X^-} \quad (5)$$

$$[Ab_{TOT}] = [AbXH] + [AbX^-] \quad (6)$$

$$1/k_{cat} = 1/k_{XH} + (1/[H_3O^+])(K_{XH}/k_{XH}) \quad (7)$$

$$1/k_{cat} = 1/(K_{XH}k_{X^-}) + (1/[H_3O^+])(1/k_{X^-}) \quad (8)$$

in D_2O. Introduction of the values of Table I in eq 7 or 8 allows derivation of the catalytic rates $k_{XH} = 9.8 \times 10^{-5}$ s^{-1} and $k_{XD} = 2.3 \times 10^{-5}$ s^{-1}, for the maximum turnover number achievable at low pH. $k_{X^-}(H_2O) = 15.5$ M^{-1} s^{-1} and $k_{X^-}(D_2O) = 8.9$ M^{-1} s^{-1} are the corresponding second-order rate constants for reaction of the antibody–substrate complex with hydronium ion. Dividing these rate constants by the second-order rate constants for the background reaction $k(H_3O^+) = 1.9 \times 10^{-3}$ M^{-1} s^{-1} and $k(D_3O^+) = 9.9 \times 10^{-4}$ M^{-1} s^{-1} gives the maximum rate acceleration factors $(k_{cat}/k_{uncat})_{max}H_2O = 8200$ and $(k_{cat}/k_{uncat})_{max}D_2O = 8900$, which are achieved at the higher pH end of the profile. The dissociation constant of the side chain in both solvents is also obtained. The corresponding negative logarithms are $pK_{XH} = 5.2$ and $pK_{XD} = 5.6$. As was already apparent from the pH-dependence of K_m, the dissociation constant K_{XH} of the antibody side chain is subject to a thermodynamic solvent isotope effect which shifts its pK_{XD} approximately 0.4 pH units higher relatively to the pK_{XH}.

Table I. pH Profile of Antibody 14D9 Catalyzed Hydrolysis of **4** in H_2O and D_2O

pH	k_{cat}, s^{-1}	K_m, μM	k_{cat}/k_{un}[d]	pD	k_{cat}, s^{-1}	K_m, μM	k_{cat}/k_{un}[d]
3.15[a]	9.33×10^{-5}	41	69	3.11[a]	2.19×10^{-5}	32	29
3.58[a]	8.55×10^{-5}	33	171	3.57[a]	2.37×10^{-5}	36	89
4.37[a]	8.82×10^{-5}	71	1090	4.19[a]	2.32×10^{-5}	40	363
4.58[a]	8.49×10^{-5}	73	1700	4.51[a]	2.30×10^{-5}	43	752
5.14[a]	5.37×10^{-5}	95	3890	5.03[a]	1.76×10^{-5}	62	1905
5.46[b]	3.38×10^{-5}	127	5130	5.53[b]	1.08×10^{-5}	99	3700
5.92[b]	1.60×10^{-5}	152	7020	6.00[b]	6.52×10^{-6}	130	6590
6.66[c]	3.13×10^{-6}	225	7520	6.64[c]	2.02×10^{-6}	148	9150
7.11[c]	1.33×10^{-6}	190	8990				

[a] All assays were performed in 100 mM NaCl in water with less than 1% acetonitrile as cosolvent at 20 °C. Product formation was followed by RP-HPLC (see Experimental Section). Buffers: 10 mM citric acid. [b] 50 mM MES. [c] 50 mM bis-tris. [d] Calculated from the second-order rate constants for the background reaction as average throughout the pH-range studied $k(H_3O^+) = 1.9 \times 10^{-3}$ M^{-1} s^{-1}, $k(D_3O^+) = 9.9 \times 10^{-4}$ M^{-1} s^{-1}. The measurement of k_{uncat} at high pH was inaccurate due to the small amount of product formed and increased by about 10% at low pH due to citrate buffer catalysis.

Kinetic Solvent Isotope Effect on Catalysis. There is a serious *caveat* for the interpretation of kinetic solvent isotope effects on protein catalyzed reactions because the protein structure may be significantly different in H_2O or D_2O.[7] In the present case, the limiting K_m values of substrate **4** with antibody 14D9 are similar in H_2O and D_2O. Furthermore, the affinity for the tight binding inhibitor **8** is unaffected by the isotopic change, as shown by the fact that the activity titration gives the same result in both solvents. We conclude that the structure of the antibody combining site is not significantly different in H_2O or D_2O and that the isotope effect on the antibody reaction can be interpreted in terms of its rate determining step. The kinetic solvent isotope effect on 14D9

$$k_{XH}/k_{XD} = (K_{XH}/K_{XD})(k_{X^-}(H_2O)/k_{X^-}(D_2O)) \quad (9)$$

catalyzed hydrolysis of **4** (eq 9) is obtained from the ratio of the rate constants in H_2O and D_2O expressed in eq 5. The effect changes by a factor of approximately 2.5, the ratio of the dissociation constants of the antibody side chain in H_2O and D_2O, depending on the rate law used to describe the reaction. The ratio $k_{XH}/k_{XD} = 4.3$, related to the first-order rate law (eq 3), is observed at the lower pH end of the profile. The ratio $k_{X^-}(H_2O)/k_{X^-}(D_2O) = 1.75$, related to the second order rate law (eq 4), accounts for the effect at high pH and is slightly smaller than the isotope effect $k_H/k_D = 1.92$ determined for the background reaction of **4** with hydronium ion. It must be once again stressed that both rate laws are equivalent and can account for the rates and isotope effects throughout the studied pH range. The pH-dependence of the apparent isotope effect therefore is not an indication for a change in mechanism.

The isotope effects of the antibody catalyzed hydrolysis of **4** can be compared to the kinetic solvent isotope effects for the formic acid catalyzed hydrolysis of ethyl vinyl ether.[8] The value reported for the isotope effect $k_{HCOOH}/k_{HCOOD} = 6.8$, corresponding to k_{XH}/k_{HD} above, can be divided by the known ratio of dissociation constants of formic acid in H_2O and D_2O, $K_{HCOOH}/K_{HCOOD} = 2.8$,[9] to give $k_{HCOO^-}(H_2O)/k_{HCOO^-}(D_2O) = 2.43$, corresponding to $k_{X^-}(H_2O)/k_{X^-}(D_2O)$ above, for the isotope effect of the reaction between ethyl vinyl ether and H_3O^+ under formate ion catalysis. This value is also slightly smaller than the isotope effect for the reaction of ethyl vinyl ether with hydronium ion

(6) (a) Jones, D. M.; Wood, N. F. *J. Chem. Soc.* **1964**, 5400. (b) Salomaa, P.; Kankaanpera, A.; Lajunen, M. *Acta Chem. Scand.* **1966**, *20*, 1790. For a recent leading reference: (a) Kresge, A. J.; Leibovitch, M. *J. Am. Chem. Soc.* **1992**, *114*, 3099.

(7) Jencks, W. P. *Catalysis in Chemistry and Enzymology*; Dover Publications Inc.: New York, 1987; pp 274–280.

(8) (a) Kresge, A. J.; Chiang, Y. *J. Chem. Soc. B* **1967**, 53. (b) Kresge, A. J.; Chiang, Y. *J. Chem. Soc. B* **1967**, 58.

(9) (a) Glascoe, P. K.; Long, F. A. *J. Phys. Chem.* **1960**, *64*, 188. (b) Bell, R. P.; Kuhn, A. T. *Trans. Faraday Soc.* **1963**, *59*, 1789.

Chart II. Enol Ether Substrates for Antibody 14D9 Catalyzed Hydrolyses[a]

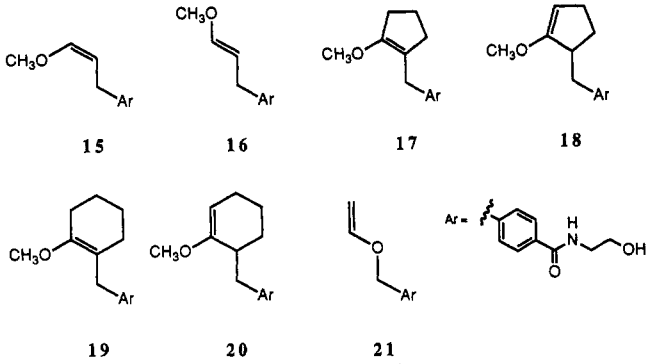

15 16 17 18

19 20 21

[a] The compounds were prepared from the acetals and ketals similarly to **4** and **5** (Scheme III and Experimental Section). See Table II for kinetic parameters.

Chart III.[a] Intramolecular Participation of Carboxyl Groups in Enol Ether Hydrolysis[10,12]

22 (general acid catalysis)

$k_{H^+}(COOMe) = 745\ M^{-1}s^{-1}$ $k_H/k_D = 2.99$
$k_{H^+}(COO^-) = 6.1\ 10^4\ M^{-1}s^{-1}$ $k_H/k_D = 1.33$
ratio: 82
$k_{AcOH}(COOMe) = 0.67\ M^{-1}s^{-1}$
$k_{AcOH}(COO^-) = 1.41\ M^{-1}s^{-1}$
ratio: 2.1

23 (substituent effect)

$k_{H^+}(COOH) = 0.22\ M^{-1}s^{-1}$ $k_H/k_D = 1.43$
$k_{H^+}(COO^-) = 46\ M^{-1}s^{-1}$ $k_H/k_D = 2.42$
ratio: 209
$k_{AcOH}(COOH) = 6.7\ 10^{-5}\ M^{-1}s^{-1}$
$k_{AcOH}(COO^-) = 1.3\ 10^{-2}\ M^{-1}s^{-1}$
ratio: 200

[a] Rate constants: k_{H^+}, second-order rate constant for the reaction with hydronium ion, k_{AcOH}, second-order rate constant for the reaction with acetic acid. The considered ionization state or chemical substitution of the carboxyl function is given in parentheses for each rate constant. All rates were measured in aqueous buffers at 25 °C (**22**) or 30 °C (**23**).

alone, $k_H/k_D = 2.95$, which corresponds to the background reaction above. In the well documented hydrolysis of the enol ether function in prostacyclin and some of its analogs like **22** (Chart III), where intramolecular general acid catalysis by the carboxyl group is operative and accounts for an 82-fold rate acceleration, an even larger reduction of the kinetic solvent isotope effect is observed:[10] $k_H/k_D = 2.99$ is reduced to $k_H/k_D = 1.33$ under intramolecular general acid catalysis.[11] For the hydrolysis of 2-ethoxy-1-cyclopentene-1-carboxylic acid (**23**) reported by Fife, the 200-fold rate accelerating effect of carboxyl ionization does not originate in general catalysis but in a simple substituent effect.[12] There, the isotope effect $k_H/k_D(COOH) = 1.43$ increases to $k_H/k_D(COO^-) = 2.42$. Thus, the reduction of the isotope effect in the antibody catalyzed reaction is consistent with the side chain operating as a general acid in the rate determining proton transfer to the β-carbon of the enol ether.

Scheme II. Possible Mechanisms for Antibody Catalyzed Protonation of **4**

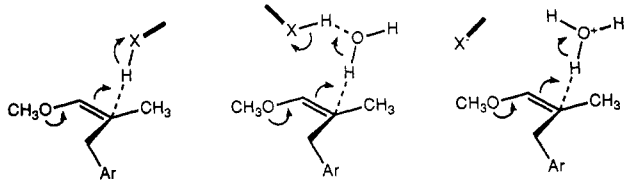

(1) (2) (3)

For the rate determining step of the antibody catalyzed reaction, which involves proton transfer to the β-carbon atom of the enol ether bound to the antibody, the unresolved mechanistic issue is whether the proton is transferred directly from H_3O^+ or by using the antibody side chain as a proton relay in an internal process within the antibody–substrate complex. Three mechanistic schemes may be envisioned that involve no more than two species in the rate determining step, namely the antibody–substrate complex and a molecule of water or the hydronium ion (Scheme II): (1) proton transfer from the side chain to the β-carbon of the enol ether; (2) proton transfer from a hydronium ion transiently bound to the side chain; and (3) proton transfer from a solvent hydronium ion with stabilization of the emerging oxocarbonium ion by the negatively charged side chain. In all three cases, electrostatic stabilization of the intermediate oxocarbonium ion (Scheme I) by AbX^- is expected to contribute to transition-state stabilization.[13]

The mechanism for proton transfer from the side chain, which is consistent with the observed isotope effect and is most probably operative in the cases of intramolecular general acid catalysis reported in the literature[14] (mechanism 1 above), seems here unlikely because it would require the protonating group to be within hydrogen bonding distance of the enol ether's β-carbon, which occupies the position of the nitrogen in the hapten. This is hardly compatible with the structural information available on antibody combining sites for quaternary ammonium ions. A model is provided by antibody McPC 603 against phosphocholine ($Me_3N^+CH_2CH_2OPO_3^{2-}$), for which a high-resolution crystal structure is available.[15] In the surrounding of the trimethylalkylammonium center, two neutralizing carboxyl groups are found. They are 4.8 and 5.8 Å away from the nitrogen center, and their orientation is such that hydrogen bonding is not possible in the direction of the nitrogen. For antibody 14D9, we have previously shown that the hydrophobic, neutral *tert*-butyl ether **9** (Chart I) is a better inhibitor ($K_i = 5\ \mu M$) than the positively charged, hydrogen bonding, primary ammonium salt **10** ($K_i = 90\ \mu M$) for the 14D9 catalyzed hydrolysis of **7**.[4] These data suggest that 14D9 does not have a hydrogen bonding group in proximity to the nitrogen center.

Substrate Variation Studies. The inhibition data cited above indicates that binding of 14D9 to hapten **1** involves van der Waals

(10) The uncatalyzed reaction is the bimolecular reaction of the neutral carboxyl compound with hydronium ion, with rate constant $k_{H^+}(RCOOH)$, and the catalyzed reaction is that of the compound with the negatively charged carboxyl group with hydronium ion, with rate constant $k_{H^+}(RCOO^-)$. Attribution of the rate acceleration effect of carboxyl ionization to general acid catalysis is established by the fact that both ionized and neutral forms have comparable reactivities toward intermolecular general acids. (a) Bergman, N. A.; Jansson, M.; Chiang, Y.; Kresge, A. J.; Yin, Y. *J. Org. Chem.* **1987**, *52*, 4449. (b) The effect is similar for the *E* isomer: Bergman, N.-A.; Jansson, M.; Chiang, Y.; Kresge, A. J. *J. Org. Chem.* **1988**, *53*, 2544. An 8-fold rate acceleration by intramolecular catalysis was reported for homoprostacyclin: Chiang, Y.; Kresge, A. J. *J. Chem. Soc., Perkin Trans. II* **1988**, 1083. Here, $k_H/k_D(RCOO^-) = 2.1$ for the catalyzed reaction. The isotope effect for the uncatalyzed neutral form ($k_{H^+} = 755\ M^{-1}\ s^{-1}$) was not reported but should be slightly higher than the value of 2.99 reported for the methyl ester of prostacyclin, which has a comparable reactivity ($k_{H^+} = 418\ M^{-1}\ s^{-1}$).

(11) Chiang, Y.; Cho, M. J.; Euser, B. A.; Kresge, A. J. *J. Am. Chem. Soc.* **1986**, *108*, 4192. The isotope effect for the neutral, uncatalyzed form was measured on the methyl ester.

(12) The rate enhancement of carboxyl ionization by substituent effect is also operative under general acid catalysis by added weak acids, e.g., acetic or formic acid, while this is not the case if the rate enhancement is caused by intramolecular general acid catalysis (see footnote 10 above). For compound **23**, hydrolysis of the enol ether function produces a β-keto acid that undergoes rapid decarboxylation under the reaction conditions to give cyclopentanone. (a) Fife, T. F. *J. Am. Chem. Soc.* **1965**, *87*, 1084. See also for comparable systems: (b) Halvarsson, T.; Bergman, N. A. *J. Org. Chem.* **1991**, *56*, 251. *J. Chem. Soc., Chem. Commun.* **1989**, 1219. (c) Kresge, A. J.; Leibovitch, M.; Sikorski, J. A. *J. Am. Chem. Soc.* **1992**, *114*, 2618.

(13) Chwang, W. K.; Eliason, R.; Kresge, A. J. *J. Am. Chem. Soc.* **1977**, *99*, 805.

(14) In all the examples cited, the direct proton transfer mechanism cannot be formally proven by the kinetic data. It, however, nicely explains the observed reduction of the kinetic solvent isotope effect upon catalysis, as discussed in detail in refs 10 and 11. In a recent publication (Ashwell, M.; Guo, X.; Sinnott, M. L. *J. Am. Chem. Soc.* **1992**, *114*, 10158), a similar reduction of the solvent isotope effect in the hydrolysis of *N*-acetylneuraminic acid was interpreted in terms of a nucleophilic participation of a carboxylate group in the stabilization of an oxocarbonium ion.

(15) Satow, Y.; Cohen, G. H.; Padlan, E. A.; Davies, D. R. *J. Mol. Biol.* **1986**, *190*, 593.

Scheme III. Synthesis of Substrates **4** and **5**[a]

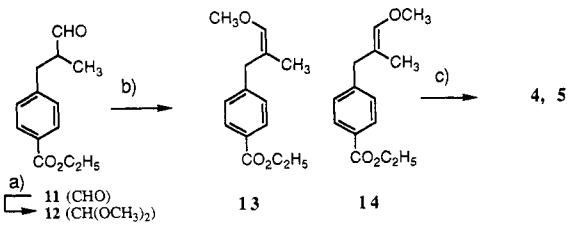

[a] Conditions: (a) $CH(OMe)_3$, MeOH, camphorsulfonic acid catalyst, 45 °C, 10 min, 93%; (b) TMSI, HMDS, CCl_4 50 °C, 4 h, then separation by chromatography on silica gel, 19% **13**, 26% **14**; (c) ethanolamine, ethanol, K_2CO_3, 50 °C, 4 h, 80%.

contacts to the hydrocarbon part of the ammonium ion, which in water provide high-binding energy due to the hydrophobic effect.[16] One would expect that these interactions, which are significantly contributing to hapten binding, should also be involved in transition-state binding and catalysis. To probe this hypothesis, we synthesized substrates **15** to **21** (Chart II), using the chemistry developed for the synthesis of substrates **4** and **5** (Scheme III and experimental part), the key reaction being the formation of the enol ether function from the corresponding acetal by reaction with iodotrimethylsilane (TMSI) and hexamethyldisilazane (HMDS).[17] To our surprise, all of them were catalytically hydrolyzed by antibody 14D9, albeit with varying efficiency. Catalyzed and uncatalyzed reaction rates for substrates **15** to **21** are reported in Table II.[18]

The absolute rates of antibody catalyzed reactions span several orders of magnitude depending on the reactivities of the substrates and the pH. This is consistent with the proton transfer being itself the rate determining step in the antibody catalyzed reaction, as was a priori accepted for the interpretation of the kinetic solvent isotope effect.

Substrate Reactivities. As shown in Table III for simple ethyl vinyl ethers, the reactivity toward H_3O^+ in water decreases with increasing β-carbon substitution. Furthermore, enol ethers of ketones react 100 times faster than enol ethers of aldehydes. This order of reactivity is expected for a late transition state resembling the oxocarbonium ion I (Scheme I) (estimates from kinetic solvent isotope effects[19] and from Bronsted coefficients[20] indicate that β-carbon–hydrogen bond formation is approximately two-thirds complete at the transition state).[21]

The second-order rate constants for enol ether protonations by H_3O^+ in water range from 10^{-2} to 10^3 M^{-1} s^{-1}. In the much faster reactions (10^9 M^{-1} s^{-1}) of enol ethers with diphenylmethyl cations, measured in acetonitrile, an exactly opposite trend is observed, with more β-substituted ethers reacting faster, and enol ethers of aldehydes and ketones having comparable reactivities[22] (Table III). This order correlates with the ionization potentials of the double bonds and was interpreted in terms of a very early transition state with no substantial geometrical change at the double bond.

One could suspect that the inverted reactivity order seen in the fast diphenylmethyl cation reactions might start to appear under antibody catalysis as an effect of the diminution of the activation energy on transition-state symmetry.[23] Such an effect could explain the observation that, for pairs of similar substrates, higher substitution at the β-carbon leads to a relatively higher catalyzed rate compared to background, as seen with **4** and **15**, **17** and **18**, and **19** and **20** (Table II, compare k_{un} rel and k_{cat} rel). Rate accelerations comparable to the antibody reaction can be obtained in 95% hexafluoroisopropyl alcohol (HFIP) with perchloric acid as catalyst.[24] As seen in Table IV, the reactivity order of substrates **4**, **5**, **15**, and **16** in this medium is however the same as in water. We conclude that the changes in the reactivity of the substrates under antibody catalysis, in particular the rate accelerating effect of β-substitution, cannot be explained by simple rate or medium effects.

Antibody 14D9 Catalyzed Reactions. As discussed above, the reactivity order of enol ethers with H_3O^+ is determined by their structure and is not sensitive to rate or medium effects. It is not affected either by general acid catalysis.[20] The effects of antibody catalysis on the reactivity order therefore have to originate in very specific interactions within the antibody binding pocket. A meaningful, quantitative measure of these antibody specific contributions to catalysis can be obtained from the rate acceleration factors k_{cat}/k_{uncat} (Table II).

In this series of substrates, a first surprise is that hydrolysis of substrates **18**, **20**, and **21** is significantly catalyzed by 14D9, although the double bond is misplaced relative to the nitrogen center in the hapten. The site of protonation is, quite unexpectedly, not crucial to catalysis. This favors a model where the ionizable side chain, which is presumably active for all substrates, exerts its catalytic effect not by direct proton transfer but mainly by interaction with the α-carbon center of the electron deficient oxocarbonium ion, which is at the same location in all substrates. This model would be compatible with transition states **2** and **3** depicted in Scheme II. By comparison, the equivalent interaction with the glycosyl cation is the accepted mode of action of one of the carboxyl side chains in the active site of glycosidase enzymes.[25]

(16) Smithrud, D. B.; Diederich, F. *J. Am. Chem. Soc.* **1990**, *112*, 339 and references cited therein.

(17) Miller, R. D.; McKean, D. R. *Tetrahedron Lett.* **1982**, *23*, 323.

(18) The enantioselectivity of these reactions is under current investigation and will be reported later. The observation of multiple catalytic turnover without deactivation with antibody 14D9 and all the substrates studied might be taken as further evidence that the ionizable side chain involved in catalysis is not in close proximity to the reacting enol ether function. In the only case of intramolecular catalysis, shown below, where the participating carboxyl group can form a stable acylal, the active side chain is alkylated by the intermediate oxocarbonium ion, which in a catalytic system would result in irreversible deactivation (Kirby, A. J.; Williams, H. N. *J. Chem. Soc., Chem. Commun.* **1991**, 1643). Here, the question of general acid catalysis versus substituent effect is, however, unresolved because solvent isotope effects and external general acid catalysis were not reported. In the case of prostacyclin and analogs discussed above, the corresponding acyl-ketal was not observed but is not expected to be stable.

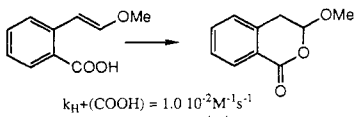

k_H+(COOH) = 1.0 10^{-2} $M^{-1}s^{-1}$
k_H+(COO⁻) = 7.97 $M^{-1}s^{-1}$
ratio: 766

(19) Kresge, A. J.; Sagatys, D. S.; Chen, H. L. *J. Am. Chem. Soc.* **1977**, *99*, 7228.

(20) Kresge, A. J.; Chen, H. L.; Chiang, Y.; Murrill, E.; Payne, M. A.; Sagatys, D. S. *J. Am. Chem. Soc.* **1971**, *93*, 413.

(21) The observed reactivity order for β-carbon substitution can be explained by differences in the thermodynamic stabilities of the ground states. Rehybridization of the β-carbon causes the stabilizing effects of β-carbon substituents on the double bond of the enol ether to disappear at the transition state. A quantitative measure of this effect is given by the decrease in heats of hydrogenation from 1-propene (–30.1 kcal/mol), to *cis*-2-butene (–28.6 kcal/mol), *trans*-2-butene (–27.6 kcal/mol), and 2-methyl-2-pentene (–26.9 kcal/mol) (values from: Roberts, J. D.; Caserio, M. C. *Basic Principles of Organic Chemistry*; W. A. Benjamin, Ed.; 1977; p 415). Thus β-carbon substituted vinyl ethers, being more stable, have higher activation energies for protonation and slower reaction rates. This is exactly what is observed, not only with differently β-substituted enol ethers but also between geometrical isomers, as seen for **15** and **16**. This is particularly striking for the isomeric pairs **17**, **18** and **19**, **20** (Table II), where each pair leads to only one oxocarbonium ion intermediate. Although this argument was advanced by Salomaa et al. (Salomaa, P.; Nissi, P. *Acta Chem. Scand.* **1967**, *21*, 1386), the reactivity differences discussed here have been misleadingly attributed to the relative stabilities of the intermediate oxocarbonium ions in the more recent literature (Okuyama, T.; Fueno, T.; Nakatsuji, H.; Furukawa, J. *J. Am. Chem. Soc.* **1967**, *89*, 5826 and ref 22). The 100-fold increase in reactivity from aldehyde to ketone enol ethers is explained by the additional transition-state stabilization provided both by hyperconjugation of a suitably oriented α-carbon substituent bond and by the stabilizing inductive effect of the α-carbon alkyl versus hydrogen substitution. Both effects are inoperative in the ground state and can only take effect in a late transition state with substantial carbon–hydrogen bond and thus oxocarbonium ion formation.

(22) Bartl, J.; Steenken, S.; Mayr, H. *J. Am. Chem. Soc.* **1991**, *113*, 7710.

(23) The effect of reaction rate on transition-state symmetry is apparent in the correlation between kinetic solvent isotope effects for hydronium ion catalyzed vinyl ether hydrolyses and the absolute value of the second-order rate constants. The isotope effect is found to increase with increasing rate, as expected for a trend toward an earlier transition state with less extensive carbon–hydrogen bond formation. See ref 19.

Table II.[h] Kinetic Parameters of Various 14D9 Catalyzed Hydrolyses[18,26]

substrate	pH, T, °C	k_{uncat}, s^{-1}	k_{cat}, s^{-1}	K_m, μM	k_{cat}/k_{un}	k_{un} rel[f]	k_{cat} rel[g]
4[a]	5.5, 37	3.8×10^{-8}	9.5×10^{-5}	340	2500	1	1
4[b]	5.9, 20	2.3×10^{-9}	1.6×10^{-5}	150	7000	0.15	0.42
5[a]	5.5, 37	2.9×10^{-8}	8.3×10^{-6}	130	290	0.77	0.087
15[c]	5.9, 37	3.5×10^{-7}	6.2×10^{-5}	250	180	23	1.64
15[c]	6.1, 20	3.2×10^{-8}	1.9×10^{-5}	200	600	3.4	0.80
16[c]	5.9, 37	3.8×10^{-8}	4.0×10^{-6}	240	180	4.0	0.11
17[d]	7.0, 20	4.2×10^{-6}	5.3×10^{-2}	315	12500	3500	17700
17[e]	6.0, 20	3.8×10^{-5}	3.9×10^{-1}	300	10250	3170	13000
18[d]	7.0, 20	7.9×10^{-6}	1.2×10^{-3}	180	150	6600	400
19[d]	7.0, 20	2.4×10^{-7}	8.8×10^{-5}	370	370	200	29
20[d]	7.0, 20	1.6×10^{-6}	1.4×10^{-4}	570	86	1300	47
21[e]	6.0, 20	4.1×10^{-7}	5.0×10^{-5}	110	120	34	1.7

[a] All assays were measured in 100 mM NaCl, 50 mM buffer in water with less than 1% acetonitrile. Product formation was followed by RP-HPLC (see Experimental Section): MES (morpholinethane sulfonic acid) pH 5.5 (37 °C). [b] MES pH 5.9 (20 °C). [c] MES pH 5.9 (37 °C), pH 6.1 (20 °C). [d] Bis-tris (bis(2-hydroxyethyl)iminotris(hydroxymethyl)methane) pH 7.0 (20 °C). [e] Bis-tris pH 6.0 (20 °C). [f] Relative second-order rate constants with hydronium ion, the reference is 0.012 M^{-1} s^{-1}. [g] Relative second-order catalytic rate constants with hydronium ion, assuming that all the catalytic antibody side chain is in the free base form X^-, the reference is 30 M^{-1} s^{-1}. [h] See Scheme I and Chart II for substrate structures.

Table III. Second-Order Rate Constants in M^{-1} s^{-1} of Representative Enol Ethers with Hydronium Ion and Carbocations

	$k(H_3O^+)$[a]	k_{rel}	$k((p\text{-}ClC_6H_4)_2C^+H)$[b]	k_{rel}	IP (eV)
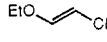	1.75	35	1.7×10^8	0.077	8.80
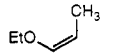	0.16	3.2	1.3×10^9	0.59	8.42
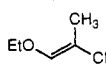	0.48	9.6	7.7×10^8	0.35	8.43
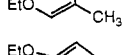	0.050[c]	1	2.2×10^9	1	8.20
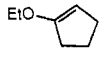	454	9080	2.5×10^9 ($OSiMe_3$)[d]	1.13	
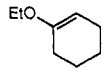	80	1600	2.3×10^9 ($OSiMe_3$)	1.05	

[a] From ref 19. Rates measured in aqueous solution at 25 °C with $HClO_4$ as catalyst. [b] From ref 22. Rates measured in acetonitrile at 20 °C. The bis(*p*-chlorophenyl)methyl cation was generated by laser flash photolysis of the corresponding chloride. [c] Estimated from the rate for the corresponding methyl ether (ref 19), substitution of ethyl for methyl doubles the protonation rate. [d] $k = 1.9 \times 10^9$ M^{-1} s^{-1} for the corresponding methyl ether.

The catalytic effect k_{cat}/k_{uncat} in substrates **18**, **20**, and **21** is very similar and ranges from 86 to 150. These numbers compare well with the effect obtained in intramolecular general acid catalysis ($k_{H^+}(COO^-)/k_{H^+}(COOH) = 83$ in the case of **22**, Chart III) and might reflect the catalytic contribution of the ionizable side chain alone.

Significantly better results are obtained with substrates **4**, **5**, **15**, **16**, **17**, and **19**. Their common structural feature is the placement of the β-carbon at the site of the haptenic nitrogen center. As can be appreciated by comparing substrate **21** and **15** (20 °C) or **16**, "inverting" the enol ether increases catalysis by a factor of 6. We see furthermore an approximately 12-fold increase[26] in catalytic efficiency between **15** and its β-methyl analog **4** and a 34-fold increase between the six membered enol ether **19** and its five-membered analog **17**.

As discussed above, these structural effects on the efficiency of the antibody 14D9 catalyzed hydrolysis of the enol ether function are not medium or intrinsic rate effects. We propose that specific van der Waals contacts to the added methyl group in **4** relative to **15** activate the double bond by pyramidalization. Such an effect is expected to result from the strong interactions between the hydrocarbon substituents of the tetrahedral quaternary ammonium hapten and the antibody, whose importance was demonstrated by the inhibition experiments cited above. Remarkably, the K_m values of **15** and **4** are very similar, which is consistent with the hypothesis that the added binding energy is not utilized for tighter substrate binding but for catalysis. The rate enhancing effect of the added methyl group therefore probably reflects the general principle of strain in catalysis.[27] In the present case, it is worth a factor of 12, or approximately 1.5 kcal/mol in transition-state stabilization. In the case of the cyclic substrates **17** and **19**, there seems to be additional interactions between the antibody active site and other parts of the cycle that either further activate (**17**) or deactivate (**19**) the substrates. Here the difference is a factor of 34 or 2.1 kcal/mol worth of transition-state stabilization. Such effects can also explain the 6-fold rate enhancement in antibody catalysis between **21**, which is unsubstituted, and the monosubstituted enol ethers **15** or **16**. Here also the K_m value increases slightly in agreement with the idea that placing the substituted, planar β-carbon in the tetrahedral environment induces strain.

In the case of the substrate pair **16**/**5**, the additional methyl group provides only a 1.6-fold enhancement in antibody catalysis. It now results in a lowering of the K_m from 230 to 130 μM, suggesting that part of the added hydrophobic interactions lost to catalysis are involved in ground-state stabilization. The 10-fold difference in rate accelerations between the *Z* and *E* isomers **4** and **5**, which is not observed with the corresponding pair **15** and **16**, is primarily the result of the very different utilization of binding energy between the antibody and the β-methyl group in these two compounds.

(24) This superacidic, highly ionizing medium is commonly used to generate carbocations. The hydrolysis rate of **4** with either perchloric acid, trifluoroacetic acid, or acetic acid increases sharply in this medium relatively to water, but drops several orders of magnitude in acetonitrile or HMPA, probably due to the deactivation of the hydronium ion by coordination to these rather basic solvents. One might argue that HFIP provides in this case a dipolar, relatively aprotic medium to which the antibody active site might be compared (Lewis, C.; Kramer, T.; Robinson, S.; Hilvert, D. *Science* **1991**, *253*, 1019). However, the rate acceleration observed in HFIP results primarily from the enhanced acidity of the hydronium ion, which is caused by the solvent's lower basicity relatively to water. The antibody, being itself in thermodynamic equilibrium with the surrounding water solvent, cannot benefit from such an effect on acidity. In fact, carboxyl groups sequestered from water in the interior of proteins are most often found to have decreased acidities (Urry, D. W.; Gowda, D. C.; Peng, S. Q.; Parker, T. M.; Harris, R. D. *J. Am. Chem. Soc.* **1992**, *114*, 8716 and references cited). In water/HFIP mixtures, the perchloric acid catalyzed hydrolysis rate is first seen to decrease from 0 to 50% HFIP and then increases sharply at higher HFIP contents (see Experimental Section). These observations suggest that the medium effect on the reaction is negative and makes in the present case a positive contribution of a medium effect in the antibody catalyzed reaction unlikely.

(25) (a) Kirby, A. J. *CRC Crit. Rev. Biochem.* **1987**, *22*, 283. (b) Sinnott, M. L. *Chem. Rev.* **1990**, *90*, 1171.

(26) As seen from the measurements with **4** and **15** at 20 °C and 37 °C, the rate acceleration effect is temperature dependent. This may reflect either a temperature dependent shift in the p*K* of the side chain or the fact that the activation parameters for catalyzed and background reactions are different. As seen in Table I, the rate acceleration k_{cat}/k_{uncat} is almost pH independent above pH 5.5, which validates the comparison of rate acceleration factors between different substrates at different pH's above 5.5.

Table IV. Hydrolysis of Substrates **4**, **5**, **15**, and **16** with Hydronium Ion in Water and 95% Hexafluoroisopropyl Alcohol (HFIP)[c]

substrate	$k_{H^+}(H_2O)$[a]	k_{rel}	k_{H^+}(HFIP)[b]	k_{rel}
4	0.012	1.3	7	1.6
5	0.0092	1	4.4	1
15	0.28	30	70	16
16	0.030	3.3	15	3.4

[a] From Table II. Rates measured at 37 °C in 100 mM NaCl, 50 mM MES, pH 5.5–5.9. [b] Rates measured in 1 mM $HClO_4$ in 95% HFIP, 5% H_2O, at 20 °C (see Experimental Section). See also footnote 24. [c] Rates in M^{-1} s^{-1}.

Conclusion

A detailed investigation of the antibody 14D9 catalyzed hydrolysis of enol ethers has been reported. The pH dependence of the catalytic rate and of the Michaelis–Menten constant for substrate **4** has been measured in H_2O and D_2O. The observed values are compatible with the direct involvement of an ionizable side chain, presumably a carboxyl group, in the antibody active site. Catalysis causes a decrease in the kinetic solvent isotope effect, as is observed with intra- and intermolecular catalyses by carboxylic acids. Whereas this decrease has been interpreted in the literature as an evidence for direct proton transfer from the general acid, this mechanism seems unlikely for the antibody because the catalytic side chain is probably not within hydrogen bonding distance of the enol ether's β-carbon.

The saturation behavior of catalysis at low pH limits the absolute catalytic rate achievable by this antibody and causes the rate acceleration factor k_{cat}/k_{uncat} to drop from a maximum of 8000 at high pH to 70 at pH 3.1, because catalysis does not keep up with the increase of the background hydronium ion reaction (Table I). We have shown that the antibody reaction can be described as a bimolecular reaction between the antibody–substrate complex bearing the negatively charged side chain and the hydronium ion. In this model, saturation of activity at low pH is due to the neutralization of an amino acid side chain, which reduces the amount of active catalyst. We predict that replacement of this amino acid, presumably aspartate or glutamate in the present case, by an amino acid bearing a more acidic group, for example, a phosphorylated serine with an acidic pK of approximately 2, should shift the saturation curve of catalytic activity to lower pH. This would allow to retain high ratios of catalysis over background at low pH where higher, practical turnover numbers in the antibody catalyzed reaction could be achieved.

Substrate variation studies show that antibody 14D9 is a surprisingly versatile catalyst. The rate accelerations depend however strongly on the substrates. This contrasts with the uniform rate accelerations observed in the super acidic medium 95% hexafluoroisopropyl alcohol with perchloric acid as catalyst.[24] Antibody catalysis can be explained by the sum of two phenomena: (1) general acid catalysis by an ionizable side chain and (2) the intervention of precise hydrophobic interactions between the substrates and the antibody binding pocket. These interactions seem to participate in catalysis in a way that does not involve substrate binding[28] but rather selectively affects transition-state stabilization. Their participation in an acid–base reaction might not have been anticipated as this type of process is usually described in terms of proton relay mechanisms. Hydrophobic forces provide the largest single contribution to antibody–antigen binding. Their involvement in catalysis is an encouraging finding for the future design of antigenic transition-state analogs for a variety of chemical transformations.[29]

This study shows that it is possible to obtain catalytic antibodies with broad substrate specificities. We have identified a number of antibodies from the original *anti*-**1,2,3** pool that catalyze the hydrolysis of benzyl vinyl ether **21** significantly better than 14D9. The aromatic group that allows for antibody recognition can in this case be linked to a variety of substituted vinyl ethers and be released after hydrolysis. We hope to develop them into reagents for enantioselective protonation with very broad substrate tolerance.

Table V. HPLC Conditions (ASAHIPAC ODP-50 (C-18 Resin), 0.8 mL/min)

substrate	eluent[a]	t_R (min)	t_R-(product)[b] (min)	ref	t_R(ref) (min)
4	77% H_2O[c]	23.4	6.9	*N*-ethyl-	10.3
(**5**)	23% CH_3CN	(19.5)		benzamide[d]	
15	80% H_2O	20.8	6.6[e]	*N*-ethyl-	14.0
(**16**)	20% CH_3CN	(21.7)		benzamide[d]	
17	70% H_2O[f]	18.9	5.5	*N*-ethyl-	7.2
(**18**)	30% CH_3CN	(20.7)		benzamide[d,g]	
19	65% H_2O	14.2	5.8	methyl 4-OH	11.2
(**20**)	35% CH_3CN	(17.8)		benzoate[h]	
21	88% H_2O	45	5.0	2(2′OHethyl)-	18
	12% CH_3CN			acetanilide[i]	

[a] Premixed eluent. Premixing allows to double the peak resolution in most cases compared to proportioning valve mixing. Retention times varied about 10% depending on the exact composition, but calibration results were unaffected. [b] The product is the corresponding carbonyl compound, for **21** it is the benzylic alcohol. [c] With 0.1% trifluoroacetic acid. [d] 4 mM stock solution was mixed with 25 mM substrate stock solution before dilution. [e] 15-μL aliquots were mixed with 15 μL of 50 mM NaCN in water and injected on the HPLC, the product observed is the corresponding cyanohydrin. Direct measurement of the aldehyde product was not possible due to varying proportions of hydrate formation. [f] With 0.03% triethylamine, necessary to avoid hydrolysis of the substrate on the column. [g] Methyl 4-hydroxybenzoate (stock 5 mM, t_R = 16.0 min) was also used. [h] 5 mM stock. [i] 2 mM stock.

Table VI. Perchloric Acid Catalyzed Hydrolysis of **4** in Water/HFIP Mixtures at 20 °C

% HFIP	0	9.5	48	86	95
k_{H^+} (M^{-1} s^{-1})	2.1×10^{-3}	1.6×10^{-3}	1.1×10^{-3}	1.9×10^{-2}	7
k_{rel}	1	0.77	0.53	8.9	3400

Experimental Section

A. Synthesis. Reagents were purchased from Aldrich or Fluka. Solvents: dichloromethane was dried over P_2O_5 when needed. Acetonitrile was dried over 3A molecular sieves when needed. All other solvents were A.C.S. grade from Fisher. All chromatographies (flash) were performed with Merck silica gel 60 (0.040–0.063 mm). TLC was performed with fluorescent Merck F254 glass plates. Reactions requiring anhydrous conditions were run under argon in vacuum flame dried glassware. NMR spectra were recorded on a Brucker AM-300 MHz instrument. MS, HRMS (high resolution mass spectra), and combustion analyses were provided by the Scripps Research Institute facility (Gary Siuzdak).

(*Z*)- and (*E*)-4-(2′-Methyl-3′-methoxy-2′-buten-1′-yl)-*N*-hydroxyethyl Benzamide (4 and 5). 3-(4′-Carbethoxyphenyl)-2-methylpropanal (**11**)[30] (1.1 g, 5.6 mmol) was treated with methanol (5 mL), trimethyl orthoformate (2 mL), and ±-camphorsulfonic acid (CSA, 30 mg) at 45 °C for 10 min. Workup (aqueous saturated $NaHCO_3/CH_2Cl_2$) followed

(27) Jencks, W. P. ref 7, pp 282–305. There is no doubt that van der Waals contacts to the substituents of the enol ether are being established upon binding of the different substrates. Throughout the series, these have very little effect on the affinity constant K_m, compared to the influence on the catalytic constant k_{cat} (Table II). If the energy released by the hydrophobic effect upon binding does not appear in stabilization of the antibody substrate complex, it has to be compensated by an equivalent amount of strain energy, either in the protein structure or in the substrate. Efficient catalysis then depends on the serendipitous, constructive utilization of this strain energy for transition-state stabilization, which is apparently the case for substrates **4** and **17** but not for **19**.

(28) The hydrophobic effect accounts for substrate binding in most antibody catalyzed reactions and provides energy for the "entropy trap" effects seen in antibody catalyzed cycloaddition and bimolecular condensation reactions.

(29) Interestingly, most antibody catalyzed reactions reported to date involve substrates that undergo geometrical changes from trigonal planar to tetrahedral at carbon centers where a tetrahedral atom is present in the hapten. The effect of placing an sp^2 center in an sp^3 environment, which in the present case accounts for a factor of 12 in rate acceleration for the addition of a single methyl group, might have been overlooked in other antibody catalyzed reactions.

(30) Chalk, A. J.; Magennis, S. A. *J. Org. Chem.* **1976**, *41*, 273 and 1206.

(31) Faulkner, D. J.; Petersen, M. R. *J. Am. Chem. Soc.* **1973**, *95*, 553.

by evaporation and drying (0.1 Torr, 100 °C, 2 h) gave **12** (1.38 g, 5.2 mmol, 93%) as a colorless oil. Treatment of **12** (1.12 g, 4.2 mmol) in CCl_4 (9 mL) at −10 °C with anhydrous hexamethyldisilazane (1.11 mL, 5.26 mmol) and iodotrimethylsilane (0.70 mL, 4.9 mmol), followed by heating (50 °C, 4 h), dilution with hexane (30 mL), and workup (aqeuous saturated $NaHCO_3$/ethyl acetate) gave a mixture of the two isomeric enol ethers **13** and **14**. Separation by flash chromatography (eluant: 1.5% ethyl acetate in hexane) gave **13** (R_f 0.2, 200 mg, 19%) and **14** (R_f 0.12, 290 mg, 26%) as colorless oils.

13 (130 mg, 0.55 mmol) was treated with ethanolamine (0.3 mL) and K_2CO_3 (50 mg) in ethanol (2 mL) at 50 °C for 4 h. After removal of the solvent (0.1 Torr, 50 °C, 30 min), the residue was purified by chromatography (CH_2Cl_2/methanol 20:1, R_f 0.25) and crystallization (CH_2Cl_2/hexane) to give **4** (110 mg, 0.44 mmol, 80%) as colorless crystals: mp 63–64 °C; ^{1}H NMR ($CDCl_3$) 7.69, 7.26 (2 dt, J = 8, 2, 2 × 2 H), 6.63 (m, 1 H), 5.90 (d, 1 H, J = 1.5), 3.83 (t, 2 H, J = 5), 3.62 (td, 2 H, J = 5, 4), 3.61 (s, 3 H), 3.42 (br s, 2 H), 2.78 (br s, 1 H), 1.45 (d, 3 H, J = 1.5). $C_{14}H_{19}NO_3$ (249.30) calcd C (67.45), H (7.68), N (5.62); found C (67.79), H (7.68), N (5.66). Similarily, **14** (209 mg, 0.89 mmol) gave **5** (195 mg, 0.78 mmol, 88%) as colorless crystals: mp 97–98 °C; ^{1}H NMR ($CDCl_3$) 7.71, 7.25 (2 dt, 2 × 2 H, J = 8, 2), 6.60 (br s, 1 H), 5.90 (sxt, 1 H, J = 1.5), 3.85 (br m, 2 H), 3.64 (td, 2 H, J = 5.5, 4.5), 3.60 (s, 3 H), 3.21 (br s, 2 H), 2.65 (br s, 1 H), 1.50 (d, 3 H, J = 1.5). Found C (67.44), H (7.51), N (5.32). NOE effects: **4** irradiation on δ = 5.90 gave +1.4% on δ = 3.83 and no effect on δ = 1.45. **5**: irradiation on δ = 5.90 gave +0.7% on δ = 1.50 and no effect on δ = 3.21.

(*Z*)- and (*E*)-4-(3′-Methoxy-2′-propen-1′-yl)-*N*-hydroxyethyl Benzamide (15 and 16). Reaction of *n*-nonyl 4-iodobenzoate (3.6 g, 9.6 mmol) with allyl alcohol (0.8 mL), triethylamine (1.34 mL) and $Pd(OAc)_2$ (14 mg) in acetonitrile (3 mL) at 100 °C for 40 min, followed by workup (HCl 0.5 N/ethyl acetate) and chromatography (hexane/ethyl acetate 5:1, R_f 0.25) yielded 3-(4′-(carbonyloxy)phenyl)propanal (1.85 g, 6.1 mmol, 64%) as a colorless oil: ^{1}H NMR ($CDCl_3$) 9.84 (t, 1 H, J = 1), 7.99, 7.28 (2 × 2 H), 4.31 (t, 2 H, J = 6.6), 3.03 (t, 2 H, J = 7.5), 2.83 (br t, 2 H, J = 7), 1.75 (br qt, 2 H, J = 7), 1.5–1.2 (m, 12 H), 0.89 (br t, 3 H, J = 7). It was immediately treated with methanol (6 mL), trimethyl orthoformate (3 mL), and CSA (20 mg) at 50 °C for 10 min. Removal of the solvent and chromatography (hexane/ethyl acetate 10:1, R_f 0.30) gave the corresponding dimethyl acetal (2.0 g, 5.7 mmol, 94%) as a colorless oil: $C_{21}H_{34}O_4$, HRMS (M + Cs)$^+$ calcd (483.1511) found (483.1522); ^{1}H NMR ($CDCl_3$) 7.96, 7.27 (2 × 2 H), 4.36 (t, 1 H, J = 6), 4.30 (t, 2 H, J = 7), 3.34 (s, 6 H), 2.74 (br t, 2 H, J = 8), 1.94 (m, 2 H), 1.76 (br q, 2 H, J = 7), 1.50–1.25 (m, 12 H), 0.89 (br t, 3 H, J = 7). This acetal (0.79 g, 2.26 mmol) in CCl_4 (15 mL) was treated at −10 °C with anhydrous hexamethyldisilazane (0.62 mL) and iodotrimethylsilane (0.39 mL). The solution was heated at 50 °C for 3 h, then diluted with ethyl acetate, and washed with aqueous saturated $NaHCO_3$ and brine. Chromatography of the residue (hexane/ethyl acetate 20:1, R_f 0.32) yielded a 1.5/1 mixture of isomeric enol ethers (205 mg, 0.64 mmol, 29%). Both isomers could be separated by three successive chromatographies (hexane/CH_2Cl_2 3:1, R_f 0.32 *Z* isomer, 0.29 *E* isomer). Reaction of the purified *Z* isomer (32 mg, 0.1 mmol) with ethanolamine (0.2 mL) and K_2CO_3 (50 mg) in ethanol (1 mL) at 50 °C for 12 h followed by chromatography (CH_2Cl_2/methanol 20:1, R_f 0.26) gave **15** (22 mg, 0.094 mmol, 93%) as a colorless oil: $C_{13}H_{17}NO_3$, HRMS (M + Cs)$^+$ calcd 368.0263, found 368.0266; ^{1}H NMR ($CDCl_3$) 7.71, 7.29 (2 td, 2 × 2 H, J = 8, 2), 6.59 (br s, 1 H), 6.05 (dt, 1 H, J = 6, 1.5), 4.55 (td, 1 H, J = 7.5, 6), 3.85 (t, 2 H, J = 5), 3.65 (s, 3 H), 3.64 (td, 2 H, J = 5, 4), 3.46 (dd, 2 H, J = 7.5, 1.5). Similarily, the *E* isomer (50 mg, 0.16 mmol) gave **16** (27 mg, 0.115 mmol, 72%) as a colorless crystalline solid: HRMS (M + Cs)$^+$ calcd 368.0263, found 368.0263; ^{1}H NMR ($CDCl_3$) 7.72, 7.29 (2 d, 2 × 2 H), 6.61 (br s, 1 H), 6.43 (dt, 1 H, J = 12.5, 1.5), 4.88 (dt, 1 H, 12.5, 7), 3.85 (br t, 2 H, J = 5.5), 3.65 (td, 2 H, J = 5, 4), 3.55 (s, 3 H), 3.32 (br d, 2 H, J = 7.5), 2.68 (br s, 1 H).

4-((2′-Methoxy-1′-cyclopenten-1′-yl)methyl)-*N*-hydroxyethyl Benzamide (17) and 4-((2′-Methoxy-2′-cyclopenten-1′-yl)methyl)-*N*-hydroxyethyl Benzamide (18). Reaction of ethyl 4-(chloromethyl)benzoate (1.5 g, 7.55 mmol) with 1-pyrrolidinocyclopentene (1.0 g, 7.4 mmol) in 30 mL of dry acetonitrile at 70 °C for 15 h, followed by workup (HCl 1 N/ethyl acetate) and chromatography (hexane/ethyl acetate 8:1, R_f 0.20) gave 0.98 g of impure 2-((4′-carbethoxyphenyl)methyl)cyclopentanone. Reaction with methanol (6 mL), trimethyl orthoformate (4 mL), and CSA (33 mg) for 30 min at 20 °C, followed by workup (aqueous saturated $NaHCO_3$/ethyl acetate) and chromatography (ethyl acetate/hexane 1:15, R_f 0.18) gave the corresponding pure dimethyl acetal as a colorless oil (0.66 g, 2.34 mmol, 31%): ^{1}H NMR ($CDCl_3$) 7.95, 7.26 (2 dd, 2 × 2 H), 4.38 (q, 2 H, J = 7), 3.30, 3.24 (2s, 2 × 3 H), 3.04 (dd, 1 H, J = 13, 3), 2.37 (dd, 1 H, J = 13, 13), 2.29 (m, 1 H), 1.93 (m, 1 H), 1.84–1.50 (m, 4 H), 1.40 (t, 3 H, J = 7), 1.30 (m, 1 H). Reaction with hexamethyldisilazane (0.62 mL) and iodotrimethylsilane (0.38 mL) in CH_2Cl_2 (15 mL) at 20 °C for 3 h, followed by dilution with hexane, workup (aqueous saturated $NaHCO_3$/ethyl acetate), and chromatography (2% diethyl ether in hexane) gave the trisubstituted isomer (R_f 0.15, 300 mg, 1.03 mmol, 44%). Two additional chromatographies were necessary to obtain the isomerically pure tetrasubstituted isomeric enol ether (R_f 0.12, 200 mg, 0.69 mmol, 29%). Reactions with ethanolamine and purification as above yielded **17** (tetrasubstituted) and **18** (trisubstituted) as colorless oils in >90% yields.

17 (tetrasubstituted): $C_{16}H_{21}NO_3$ HRMS (M + Cs)$^+$ calcd 408.0576, found 408.0588; ^{1}H NMR ($CDCl_3$) 7.68, 7.22 (2 dt, 2 × 2 H, J = 8, 2), 6.72 (br t, 1 H), 3.81 (dd, 2 H, J = 6, 5), 3.63 (s, 3 H), 3.60 (dd, 2 H, J = 6, 4.5), 3.4 (br s, 2 H), 2.48, 2.10, 1.81 (3 m, 3 × 2 H).

18 (trisubstituted): HRMS (M + Cs)$^+$ found 408.0588; ^{1}H NMR ($CDCl_3$) 7.70, 7.25 (2dd, 2 × 2 H), 6.60 (br, 1 H), 4.47 (q, 1 H, J = 2), 3.85 (q, 2 H, J = 5), 3.65 (td, 2 H, J = 5.5, 4), 3.64 (s, 3 H), 3.05 (dd, 1 H, J = 13.5, 4), 2.89 (m, 1 H), 2.65 (br t, J = 4, 1 H), 2.56 (dd, 1 H, J = 13.5, 9), 2.12 (m, 2 H), 1.91 (m, 1 H), 1.54 (m, 1 H).

4-((2′-Methoxy-1′-cyclohexen-1′-yl)methyl)-*N*-hydroxyethyl Benzamide (19) and 4-((2′-Methoxy-2′-cyclohexen-1′-yl)methyl)-*N*-hydroxyethyl Benzamide (20). 2-(Ethoxycarbonyl)cyclohexanone (1.0 g, 5.9 mmol) was added to a solution of NaH (225 mg 60% in oil, 5.6 mmol) in 18 mL of absolute ethanol. Ethyl 4-(chloromethyl)benzoate (0.8 g, 4 mmol) was added, and the solution was heated at 60 °C for 5 h. Workup (aqueous saturated NH_4Cl/ethyl acetate) and chromatography (hexane/ethyl acetate 10:1, R_f 0.5) gave 1.13 g of a crude product which was treated with acetic acid/concentrated HCl 5:1 at reflux for 24 hours. The acid was removed by coevaporation with toluene, and the residue was treated with methanol (30 mL) and thionyl chloride (1 mL) at 50 °C for 2 h. Workup (aqueous saturated $NaHCO_3$/ethyl acetate) and chromatography (10% ethyl acetate in hexane, R_f 0.20) gave 2-((4′-carbomethoxyphenyl)methyl)cyclohexanone (0.31 g, 1.26 mmol, 23%). Reaction with methanol (6 mL), trimethyl orthoformate (3 mL), and CSA (30 mg) at 30 °C for 15 min, followed by workup (aqueous saturated $NaHCO_3$/ethyl acetate) and chromatography (hexane/ethyl acetate 15:1, R_f 0.10), gave the corresponding dimethyl acetal (0.35 g, 1.2 mmol, 95%): ^{1}H NMR ($CDCl_3$) 7.96, 7.25 (2 dt, 2 H, J = 8, 2), 3.91, 3.26, 3.21 (3s, 3 × 3 H), 2.90 (dd, 1 H, J = 14, 3.5), 2.61 (dd, 1 H, J = 14, 12), 2.16 (m, 1 H), 1.84 (m, 1 H), 1.63 (m, 1 H), 1.58–1.26 (m, 6 H). Reaction with hexamethyldisilazane (0.34 mL) and iodotrimethylsilane (0.21 mL) in CH_2Cl_2 (10 mL) at 20 °C for 6 h, followed by workup (aqueous saturated $NaHCO_3$/ethyl acetate) and chromatography (4% diethyl ether in hexane) gave the trisubstituted enol ether (R_f 0.20, 174 mg, 0.67 mmol, 56%) and the tetrasubstituted enol ether (R_f 0.13, 127 mg, 0.49 mmol, 41%). Reactions with ethanolamine and purification as above gave **19** (tetrasubstituted, 117 mg, 0.4 mmol, 83%) and **20** (trisubstituted, 183 mg, 0.63 mmol, 94%) as colorless oils.

19: $C_{17}H_{23}NO_3$ HRMS (M + Cs)$^+$ calcd 422.0732, found 422.0748; ^{1}H NMR ($CDCl_3$) 7.68, 7.25 (2td, 2 × 2 H), 6.60 (br s, 1 H), 3.83 (br q, 2 H, J = 5), 3.63 (td, 2 H, J = 5, 4.5), 3.55 (s, 3 H), 3.45 (br s, 2 H), 2.71 (t, 1 H, J = 5), 2.20, 1.86, 1.68, 1.50 (4 m, 2 × 2 H).

20: $C_{17}H_{23}NO_3$ HRMS (M + Cs)$^+$ calcd 422.0732, found 422.0732; ^{1}H NMR ($CDCl_3$) 7.70, 7.25 (2dt, 2 × 2 H), 6.61 (br, 1 H), 4.67 (t, 1 H, J = 4), 3.84 (q, 2 H, J = 5), 3.64 (td, 2 H, J = 5, 4.5), 3.15 (dd, 1 H, J = 13, 3.5), 2.70 (t, 1 H, J = 5), 2.56 (dd, 1 H, J = 13, 10), 2.44 (m, 1 H), 2.05 (m, 2 H), 1.80–1.53 (m, 4 H).

4-((Vinyloxy)methyl)-*N*-hydroxyethyl Benzamide (21). Methyl (4-hydroxymethyl)benzoate (0.262 g, 1.58 mmol) was treated with $Hg(OAc)_2$ (0.386 g) in ethyl vinyl ether (10 mL) at reflux for 24 h and for 1 additional h at 20 °C after addition of 1 mL of acetic acid.[31] Workup (aqueous saturated $NaHCO_3$/ethyl acetate) and chromatography (10% diethyl ether in hexane, R_f 0.30) gave 190 mg of methyl ((4-vinyloxy)methyl-)benzoate (0.99 mmol, 63%). Reaction with ethanolamine as above and chromatography (CH_2Cl_2/MeOH 10:1, R_f 0.20) gave 188 mg of **21** (0.85 mmol, 86%) as a colorless crystalline solid. The sample was recrystallized from CH_2Cl_2/hexane at −20 °C: mp 96–97 °C; $C_{12}H_{15}NO_3$ (221.20) calcd C (65.14), H (6.83), N (6.33); found C (65.03), H (7.01), N (6.22); ^{1}H NMR ($CDCl_3$) 7.80, 7.44 (2 td, 2 × 2 H, J = 8, 2), 6.62 (br s, 1 H), 6.58 (dd, 1 H, J = 14.5, 6.5), 4.82 (s, 2 H), 4.31 (dd, 1 H, J = 14.5, 2), 4.12 (dd, 1 H, J = 6.5, 2), 3.86 (q, 2 H, J = 5), 3.66 (td, 2 H, J = 5.5, 4.5), 2.54 (t, 1 H, J = 5).

***N*-((4′-((Hydroxyethyl)carbamido)phenyl)methyl)-*N*-methylpiperidinium Chloride (8).** 4-(Chloromethyl)benzoic acid (2.5 g, 14.7 mmol) was

suspended in CH_2Cl_2 (25 mL) and treated with oxalyl chloride (2 mL, 23 mmol) with DMF catalyst (0.03 mL) at 20 °C for 30 min. Evaporation of the solvent under vacuum left a crystalline residue which was dissolved in CH_2Cl_2 (20 mL) and treated with ethanolamine (1.8 mL, 20 mmol). Workup (brine/ethyl acetate) followed by crystallization of the residue (ethanol/hexane) gave 2.3 g (10.8 mmol, 73%) of 4-(chloromethyl)-*N*-(2′-hydroxyethyl)benzamide as colorless crystals: mp 111–112 °C; $C_{10}H_{12}ClNO_2$ calcd C (56.21), H (5.66), N (6.56); found C (56.21), H (5.68), N (6.56). Thirty milligrams of this compound (0.14 mmol) was heated with excess *N*-methylpiperidine (0.2 mL) in water (3 mL) at 80 °C for 1 h. After removal of the solvent, recrystallization from isopropyl alcohol (3 mL) and diethyl ether (5 mL) gave 23 mg (0.074 mmol, 53%) of **8**, colorless crystals: mp 233–234 °C dec; $C_{16}H_{25}N_2O_2Cl$ (312.874) calcd C (61.42), H (8.05), N (8.45); found C (60.99), H (7.82), N (8.78); ^1H NMR (D_2O) 7.84, 7.63 (2 d, 2 × 2 H), 4.55 (s, 2 H), 3.76 (t, 2 H, J = 5.5), 3.53 (t, 2 H, J = 5.5), 3.37 (m, 4 H), 2.97 (s, 3 H), 1.92 (m, 4 H), 1.72, 1.62 (2m, 2 × 2 H).

B. Kinetic Measurements. Substrates. All substrates were diluted with 1:1 acetonitrile/1 mM NaOH in water to 25 mM stock solutions and checked by HPLC for contamination by product or isomeric enol ethers. **4**, **5**, **15**, **16**, and **21** were >99.7% isomerically pure and totally free of product. **17** and **18** contained 0.2% and 1.5% product and were approximately 99.8% isomerically pure. **19** and **20** both contained 0.3% product and were 99.9% isomerically pure.

Assay Setup. All antibody solutions and buffers (Tables I and II) used were filtered through 0.22 μm micropore filters before use. For each measurement set, an antibody stock solution (5–8 mg/mL as determined by UV 280 nm, purified to homogeneity (SDS PAGE) by DEAE and Protein G chromatography as described before[4]) in the proper buffer was diluted to give approximately 1.2 mL of solution at the appropriate assay concentration (0.1–1.5 mg/mL), and 115 μL aliquots in Eppendorf tubes were prepared. A series of aliquots containing buffer only was also prepared. Sixty microliters of a solution of substrate (25 mM in acetonitrile/1 mM NaOH 1:1) was mixed with 60 μL of the appropriate internal standard stock solution in water (Table V). This solution was further diluted with water to give final concentrations of substrate 12.5 times the desired assay concentration. Six substrate concentrations spanning at least one order of magnitude were chosen between 15 and 500 μM in each setup depending on the K_m of the substrate, and the two lowest concentrations were duplicated. A 250-μL solution of inhibitor **8** was used at this point to prepare three solutions for active site titrations, which were usually performed at 100 μM substrate. Incubation was started by adding 10 μL of these diluted substrate solutions to the 115-μL aliquots of antibody or buffer only solutions, mixing with a vortex shaker and shortly centrifugating. The tubes were kept in closed plastic boxes with a wet paper towel inside for humidity saturation, at the desired temperature (37 °C or 20 °C).

Calibration. A solution of product was prepared by treating a known amount of the substrate stock solution at pH 2.0 (0.1% trifluoroacetic acid in water) until completion of the reaction, which was in all cases very clean and gave only the expected carbonyl product. This solution was diluted and compared with the chosen internal standard solution at concentrations corresponding to the real assay (0–15 μM product). The peak height and peak area ratios between product and internal reference were found to be both linearly proportional to the calculated product concentration, from zero. Better results were usually obtained using peak height measurement in the assays.

HPLC Assays. Product formation below 5% conversion versus internal reference was followed over time by reverse phase high performance chromatography (RP-HPLC) on a ASAHIPAC ODP-50 (C-18 type) column (0.45 × 22 cm) using isocratic elution at 0.8 mL/min with a premixed acetonitrile/water solvent with the desired proportion (Table V). The detection was done by UV at 254 or at 240 nm, and the signal was recorded on a digital integrator.

Data Treatment. The uncatalyzed reaction rate was calculated as an average from the rates measured in the different "buffer only" assays at different concentrations and then substracted from each antibody assay. The net rates obtained were used to derive the Michaelis–Menten constant K_m and the maximum velocity V_{max} from the Lineweaver–Burk plot of $1/V$ vs $1/[S]$. The lines were constructed from 6 to 8 points and gave correlation coefficients $0.990 < r^2 < 1.000$. The catalytic constant k_{cat} was obtained by dividing V_{max} by the measured binding site concentration as determined from the activity titration with inhibitor **8** at 100 μM substrate (4 points, $0.95 < r^2 < 1.000$). When the same antibody stock was used for a series of assays, an average of the measured binding site concentrations was used for the calculation throughout the series. For substrate **17** to **20**, the active site concentration was derived from a measurement of the same antibody stock solution with substrate **18**. For the measurement of **17** and **21** at pH 6.0, the active site concentration was taken from a measurement of the same stock with **4**. With all substrates, the reaction was quantitatively inhibited by **8**.

pH-Profile with Substrate 4. An antibody stock in PBS (50 mM phosphate pH 7.4, 100 mM NaCl) was dyalized four times in 25 mM MES pH 5.5, 100 mM NaCl in water or D_2O. The final antibody stock concentration was 5.0 mg/mL (UV, 280 nm) in both cases. The following buffers were prepared: 10 mM citric acid, 100 mM NaCl at pH 3.0, 3.5, 4.0, 4.5, 5.0, 50 mM MES, 100 mM NaCl at pH 5.5, 6.0, 50 mM bis-tris, 100 mM NaCl at pH 6.7, 7.2. The antibody stock solution (100 μL) was mixed with each buffer (1.1 mL). The uncatalyzed reaction was measured in the corresponding buffer mixture without the antibody, whose pH was measured.

Measurements in D_2O. All pH-meter readings in D_2O were corrected to 0.4 pH unit higher to obtain the pD value. D_2O (99.8% pure) from Aldrich was used. Aliquots (10-mL) of each buffer in water were lyophilized and then dissolved in 10 mL of D_2O, and the pD was adjusted with DCl/NaOD as needed. The 25 mM substrate and 4 mM reference stocks in H_2O were used but diluted with 99.8% D_2O. The H_2O content in the highest concentrated assay (500 μM) is 3% and below 1% in the diluted assays.

In the pH-profile, approximately 30% higher binding site concentrations were measured at the low pH (pH 3.1–4.2) in both water and D_2O, which was attributed to a significant decrease of the affinity of **8** for the antibody at low pH (pD). For these measurements, the binding site concentration of the antibody stock used throughout the profile was taken from an average from the measurement at pH (pD) 5.0, 5.5, and 6.0. Antibody stocks in H_2O and D_2O were from the same batch and gave the same ratio of binding site to milligrams of protein (from UV 280 nm).

Relative Rates in HFIP (Hexafluoroisopropyl Alcohol). $HClO_4$ (0.7 mM) in HFIP was prepared by diluting 70% $HClO_4$ in water with 99% pure HFIP (Aldrich). Three stock solutions in water were prepared containing each 1.3 mM *N*-ethylbenzamide as internal reference and 8.3 mM of each: (1) **4** and **15**, (2) **4** and **16**, and (3) **5** and **16**. The reactions were started by adding 5 μL of a stock solution to 95 μL of 1 mM $HClO_4$ in HFIP. Aliquots (5 μL) were taken at 5–10-s intervals and mixed with 40 μL of 50 mM NaCN in water (pH 9.0) to stop the reaction. Product formation was measured by RP-HPLC as above over 2–3 half-lives, and the data were treated as first-order kinetics. The absolute rates obtained are somewhat inaccurate due to the short reaction times (5–20 s) for manual pipetting and the sensitivity of the rate to the water content. However, the relative values obtained by mixed assays are reliable. The hydrolysis rate of **4** in a function of water content was measured with 7 mM $HClO_4$ (0.1%).

Acknowledgment. We thank Prof. A. J. Kresge and Prof. D. Hilvert for helpful suggestions and Prof. E. Keinan for critical reading of the manuscript. We thank the Fonds National Suisse pour la Recherche Scientifique for financial support (J.-L.R.).